

The contribution of remotely sensed data to the stress state evaluation in underground marble quarries

Original

The contribution of remotely sensed data to the stress state evaluation in underground marble quarries / Bonetto, Sabrina Maria Rita; Vagnon, Federico; Umili, Gessica; Vianello, Davide; Migliazza, Maria; Ferrero, Anna Maria. - In: THE EGYPTIAN JOURNAL OF REMOTE SENSING AND SPACE SCIENCES. - ISSN 1110-9823. - 24:1(2021), pp. 1-13. [10.1016/j.ejrs.2020.12.008]

Availability:

This version is available at: 11583/2960763 since: 2022-04-07T18:13:32Z

Publisher:

Elsevier

Published

DOI:10.1016/j.ejrs.2020.12.008

Terms of use:

This article is made available under terms and conditions as specified in the corresponding bibliographic description in the repository

Publisher copyright

(Article begins on next page)

HOSTED BY



Contents lists available at ScienceDirect

The Egyptian Journal of Remote Sensing and Space Sciences

journal homepage: www.sciencedirect.com

Research Paper

The contribution of remotely sensed data to the stress state evaluation in underground marble quarries

Sabrina Maria Rita Bonetto^a, Federico Vagnon^{a,*}, Gessica Umili^a, Davide Vianello^a, Maria Rita Migliazza^b, Anna Maria Ferrero^a^a Università degli Studi di Torino, Department of Earth Sciences, 10125 Turin, Italy^b Politecnico di Torino, Department of Structural, Geotechnical and Building Engineering, 10129 Turin, Italy

ARTICLE INFO

Article history:

Received 30 May 2020

Revised 30 November 2020

Accepted 26 December 2020

Keywords:

Carrara marble

Paleostress

Structural geology

Lineament extraction

ABSTRACT

An in-depth knowledge of the geostructural characteristics of the territory is fundamental for optimizing the design of artificial structures. Feasibility, costs, duration, and issues of the works are strictly correlated with the geological, geomechanical, and in situ stress features of the area. Remotely sensed data represent a source of information for detecting tectonic structures that can be complementary to traditional surveys, with the advantage of being cheaper, of covering large areas and of reducing time for surveying. The study of the regional tectonic setting together with local structural features is fundamental to define the far-field tectonic stress and for correctly modeling the induced stress during excavation activities and monitoring stress variations. A multiscale and multidisciplinary approach was set up and applied to an area in the Alpi Apuane marble district (Tuscany, Italy). Visually and semi-automatically detected geological structures were analyzed and correlated to data from in-situ measurements in four underground marble quarries, to define the far-field stress state. This study is also an attempt to bridge the gap between structural geology analysis and remotely sensed data for far-field stress definition, correlating on-field kinematic observations and in situ stress measurements.

© 2020 National Authority for Remote Sensing and Space Sciences. Production and hosting by Elsevier B.V. This is an open access article under the CC BY-NC-ND license (<http://creativecommons.org/licenses/by-nc-nd/4.0/>).

1. Introduction

Tectonic structures such as faults, large-scale fractures, and fracture zones play an important role in many geological, hydrogeological, mining, and geoenvironmental fields. In-depth knowledge of the geostructural aspects is fundamental for optimizing the design of artificial structures. The preliminary design requires to consider both the areal extent of the structure and its surroundings, to identify geological and tectonic features and their possible interactions with the structure. In many cases, traditional surveys do not provide exhaustive coverage of the study area, due to the inaccessibility of the sites and the high investigation costs.

Digital Terrain Models (DTM) can be used as shaded relief models either alone (Seleem, 2013) or in combination with aerial images at a regional scale (Jacques et al., 2012).

For these reasons, the spreading of automatic or semi-automatic methods for regional-scale analysis is encouraged by many authors (Ganas et al., 2005; Ramli et al., 2010; Masoud and Koike, 2011; Vaz et al., 2012; Soto-Pinto et al., 2013; Al-Obeidat et al., 2016 (Ferrero et al., 2016)), coupled with on-site surveys for validating and integrating the results.

The local stress field derives from the far-field tectonic stress, also known as “far-field boundary conditions” (Maerten et al., 2016), and it is an essential parameter for the definition of the geomechanical model. Unfortunately, it is not possible to directly measure past tectonic stresses, but a rough reconstruction of their orientation can be made by analyzing geological structures.

Focusing on underground works, their design and stability are strictly influenced by the local and regional stress field, in addition to rock mass properties.

Since the exact evaluation of the natural stress state is not possible (Amadei and Stephansson, 1997), methods of paleostress analysis from faults data (particularly fault-slip data) have been

Peer review under responsibility of National Authority for Remote Sensing and Space Sciences.

* Corresponding author.

E-mail addresses: sabrina.bonetto@unito.it (S.M.R. Bonetto), federico.vagnon@unito.it (F. Vagnon), gessica.umili@unito.it (G. Umili), davide.vianello@unito.it (D. Vianello), maria.migliazza@polito.it (M.R. Migliazza), anna.ferrero@unito.it (A.M. Ferrero).

<https://doi.org/10.1016/j.ejrs.2020.12.008>

1110-9823/© 2020 National Authority for Remote Sensing and Space Sciences. Production and hosting by Elsevier B.V.

This is an open access article under the CC BY-NC-ND license (<http://creativecommons.org/licenses/by-nc-nd/4.0/>).

successfully used in the last five decades. The regional tectonic stress strongly influences faults and fractures, and this is the reason why most of the studies that aim to characterize the stress system analyze orientation, interaction and fracture mode (opening, closing, shearing) of faults (Angelier, 1994; Lisle et al., 2001; Célérier et al., 2012; Fossen, 2016).

Morphology and local geological structures can modify the orientation of the main stress tensors of the regional stress field (Rawnsley et al., 1992; Maerten et al., 2016), and they need to be considered in the planning stage and the monitoring activities.

Thus, combining far-field tectonic stress, local geological structures, and morphology becomes fundamental for correctly

modeling the induced stress during excavation activities, planning the in-situ measurements, and monitoring stress variations.

In this paper, the authors present an example of regional tectonics analyzed on DTM, in association with on-site geostructural characterization, for the far-field stress definition. The results are integrated with in-situ stress measurements to point out the local stress field and its modifications induced by the quarry excavation.

The methodology is applied to four underground quarries located in the Alpi Apuane marble district (Tuscany, Italy), named Piastriccioni, Fantiscritti, Ravaccione, and Piastreta quarry.

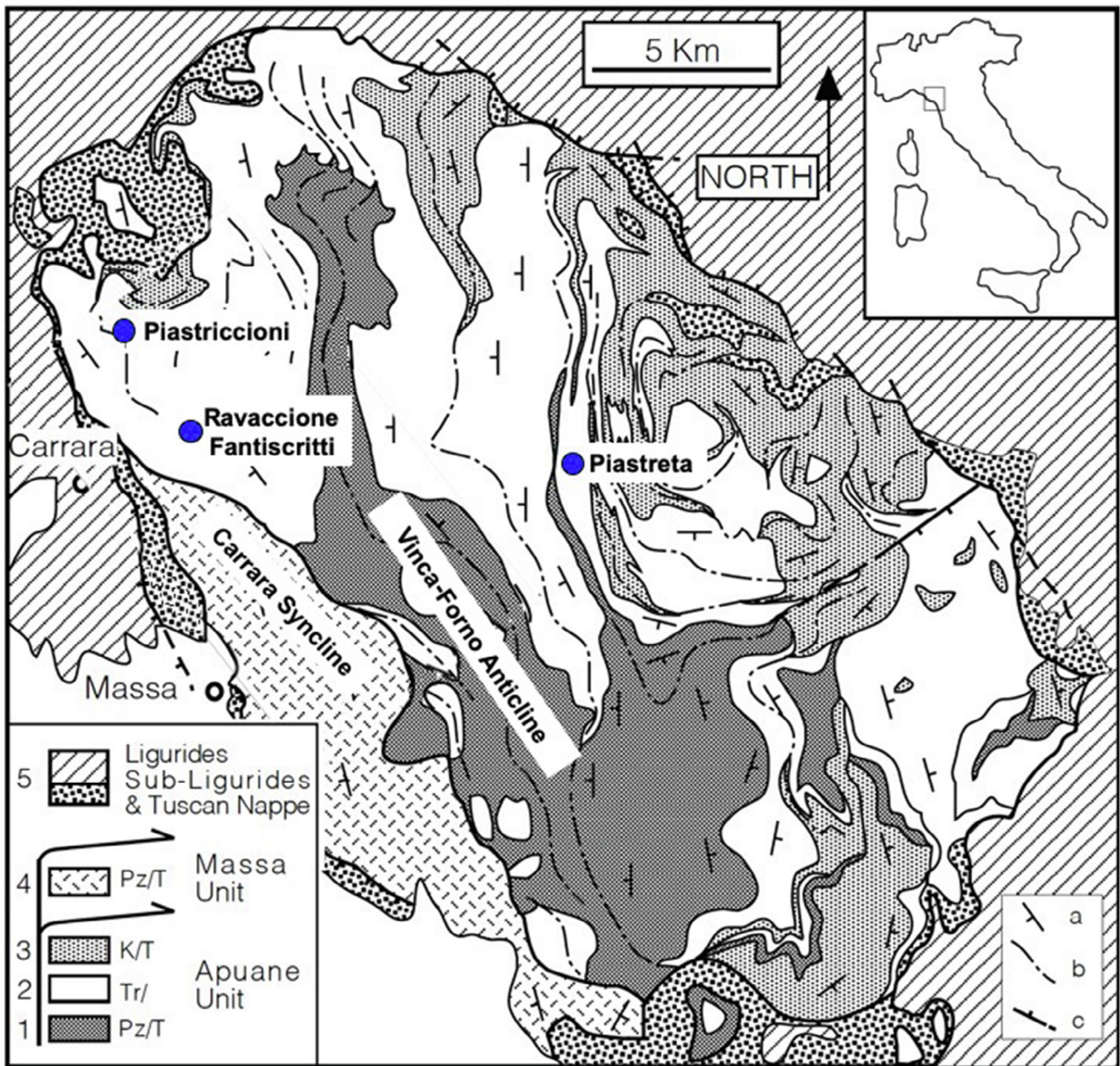


Fig. 1. Geographical location and geological map of the study area (modified from Molli et al., 2002).

2. Geographical and geological settings

The Alpi Apuane belong to the northern Apennine (NW Tuscany, Italy) and include four tectonic units: the Liguride and sub-Liguride systems, the Tuscan Nappe (TN), the Massa Unit (MU) and the Apuane Unit (AU). They represent a tectonic window in which the deepest outcropping rocks belong to the AU and the MU, which are polideformed metamorphic units and constitute the Apuane Metamorphic Complex (Molli et al., 2002). In detail, AU (Fig. 1) comprises a Paleozoic basement, Upper Triassic to Liassic carbonate platform deposits, Dogger to Tertiary calcschists, metacherts, phyllites, and metasandstones.

In particular, the well-known Carrara Marble derives by the greenschist facies metamorphism of the carbonate Liassic platform deposits (Marmi s.s. Formation) (Molli et al., 2002).

According to Carmignani and Kligfield (1990), in the Alpi Apuane, two deformation phases, D1 and D2, can be recognized. In particular, in the AU, during D1 contractional tectonics, isoclinal northeastward folds and widespread stretching lineation (L1) were developed. The so-called Carrara Syncline and the Vinca-Forno Anticline are the most famous D1 folds in the studied area, with axis trending NW-SE and axial plane schistosity (S1) dipping to SW.

Subsequent deformation events (D2) happened with an early D2 stage, with west-vergent folds, associated with a low dipping to sub-horizontal axial planar foliation (S2), and a late D2 stage of folds with a sub-vertical axial plane and high angle normal and transcurrent faults (Ottria and Molli, 2000).

The four marble quarries analyzed in this study belong to the AU. Since Ravaccione and Fantiscritti quarries belong to the same mining district and they are close to each other (Fig. 1), in the following, they will be included in a unique area.

All the quarries are exploited with the room and pillar excavation technique in the underground environment using diamond wire saws and/or marble chainsaws. The average height of Piastreta underground caverns is 8 m, while the other quarries have higher caverns (20–25 m).

3. Methodology

A multiscale and multidisciplinary approach was set up to define the far-field stress state of the area in which the four quarries are located.

At a regional scale, the lineament extraction was performed on three rectangular DTMs (area of about 10 km²), using regional DTM (GEOscopio, <http://www.regione.toscana.it/-/geoscopio>), with a resolution of 10x10m. The results were compared with the literature data.

These databases were then integrated with data obtained from traditional geostructural surveys carried out in the quarries. In situ stress measurements were carried out in the same quarry areas and compared with regional and local structural data.

In the next sections, a brief description of the methodologies is provided.

3.1. Lineament extraction

3.1.1. The semi-automatic approach (SAA)

CurvaTool code is based on the calculation of principal curvature values for each point of a 3D digital model, as indexes of local convexity and concavity of the surface, respectively.

The original code was modified for identifying linear features on DTMs representing portions of the territory and was tested on different case studies (Bonetto et al., 2017; 2020; Umili et al., 2018).

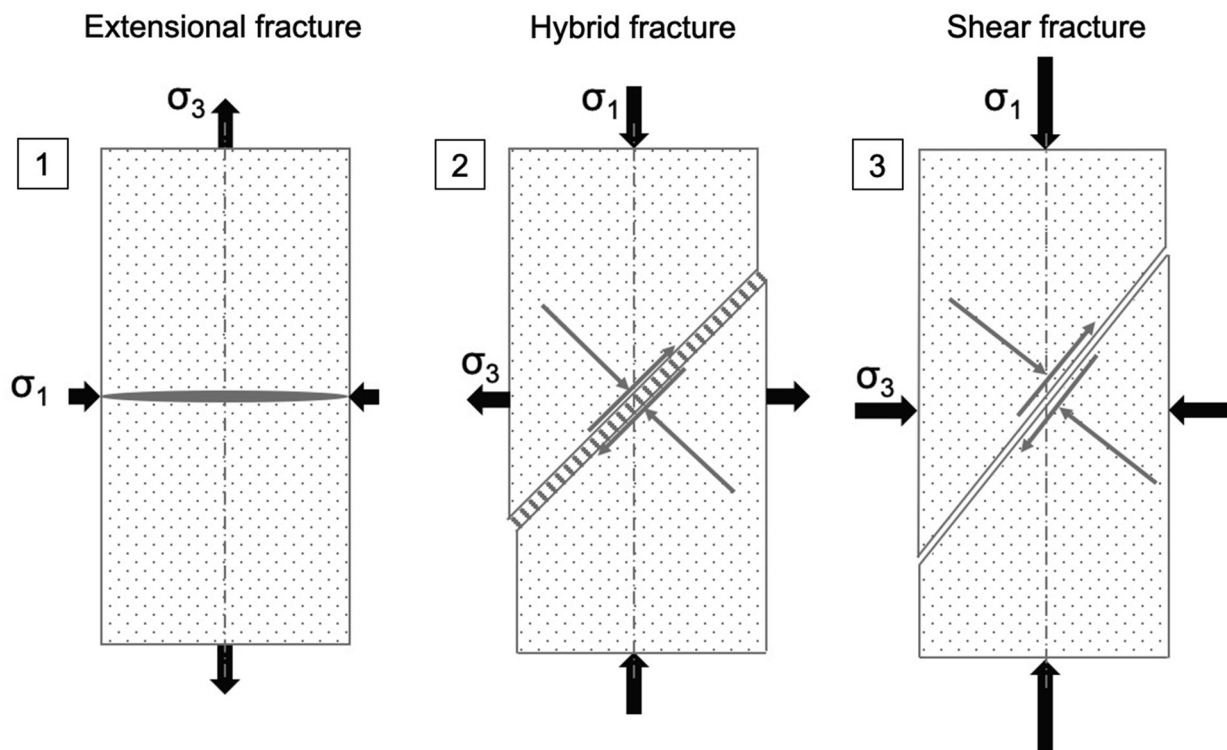


Fig. 2. Schematic representation of fracture types and relationships with principal stress axes (modified from Cosgrove and Hudson, 2016).

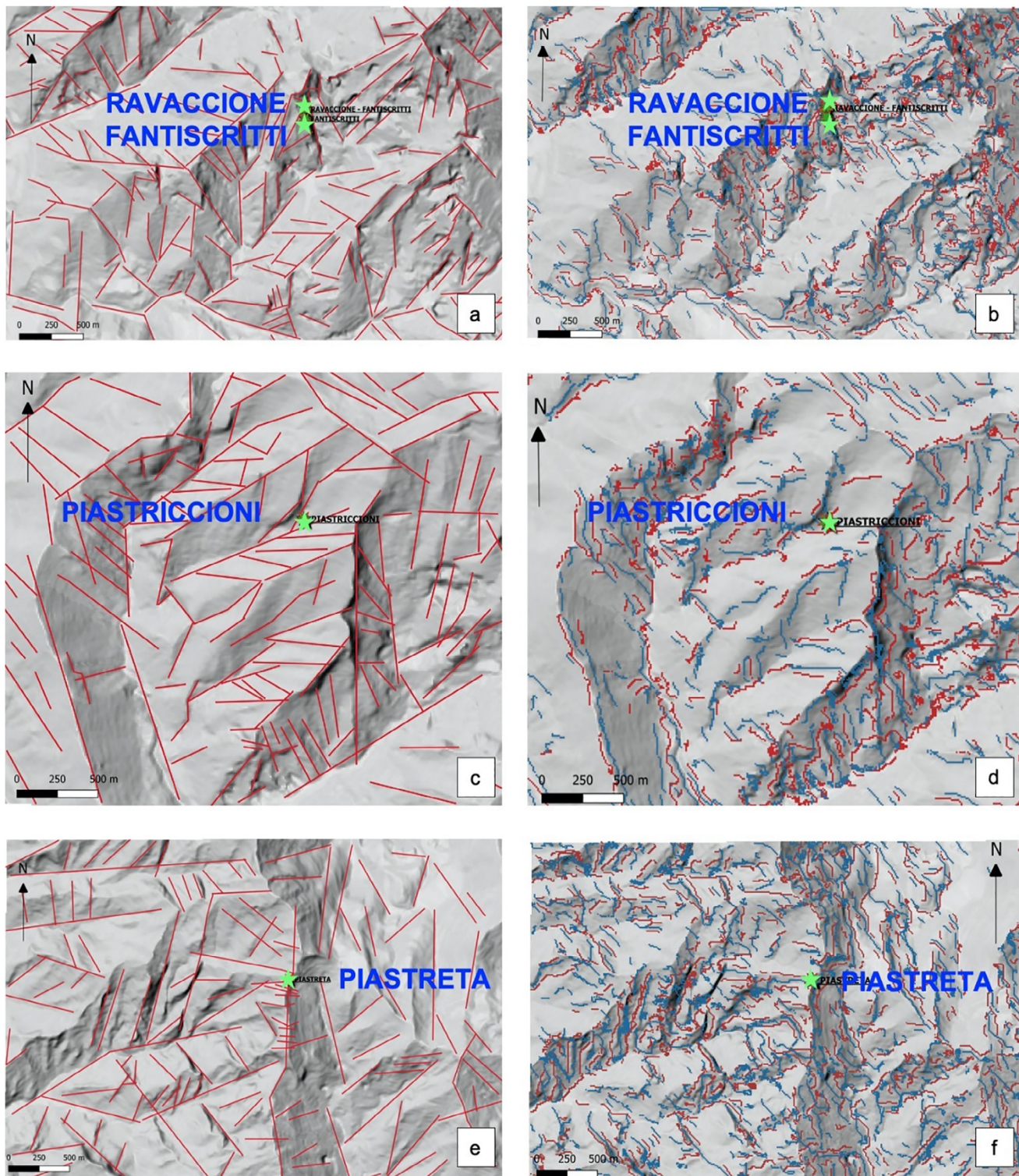


Fig. 3. Lineament extraction results from VA (a, c, e) and SAA (b, d, f) approaches.

Table 1
Results of VA and SAA approaches in terms of number and total length of detected linear features.

| Pertaining area | Surface area [km ²] | Visual approach | | Curva Tool Code | |
|-------------------------|---------------------------------|-------------------------------|-------------------|-------------------------------|-------------------|
| | | Number of linear features [-] | Total length [km] | Number of linear features [-] | Total length [km] |
| Fantiscritti-Ravaccione | 10.44 | 250 | 64.94 | 871 | 119.82 |
| Piastriccioni | 8.27 | 176 | 57.08 | 607 | 83.75 |
| Piastrreta | 11.77 | 154 | 58.03 | 1016 | 139.29 |

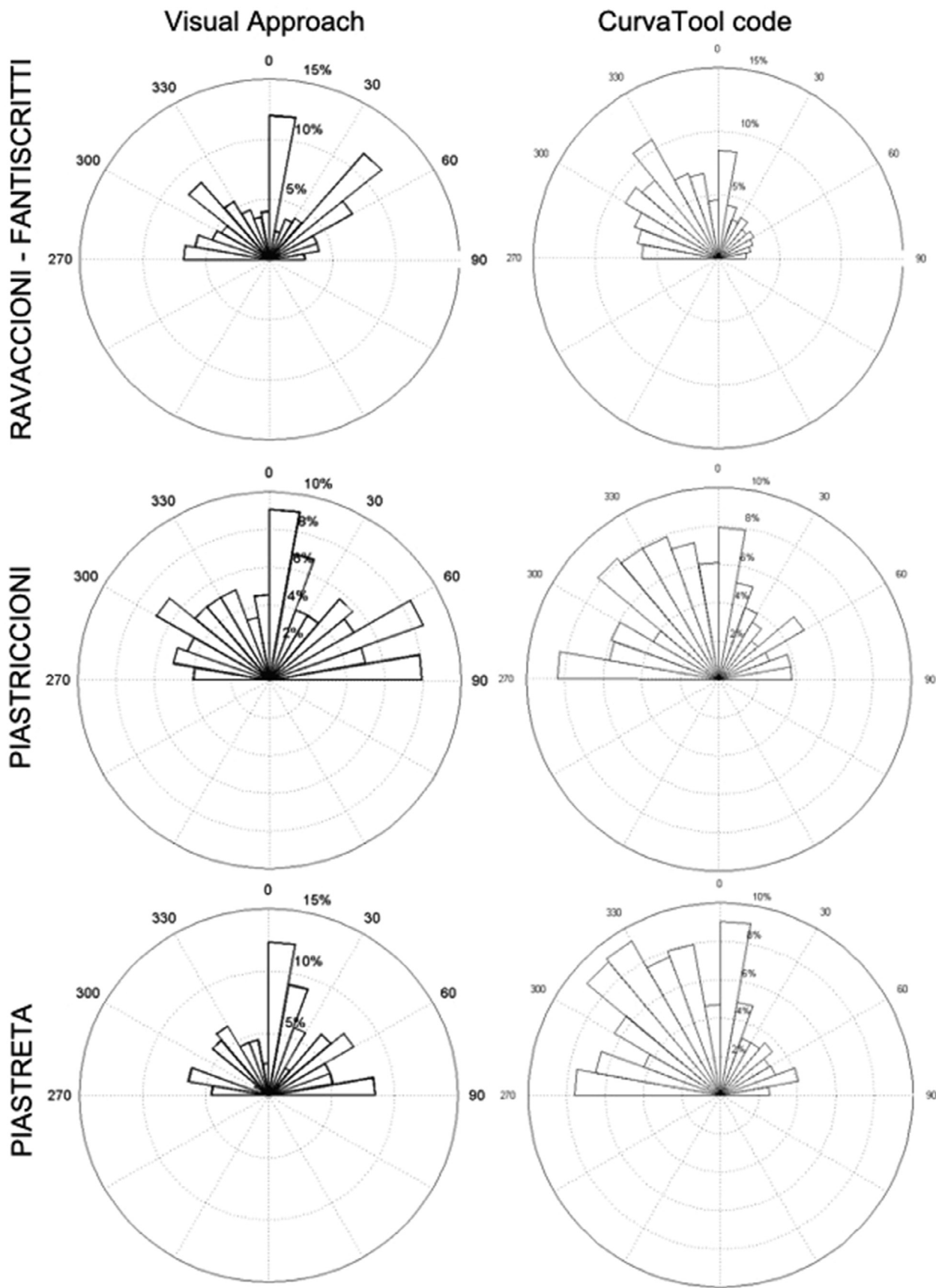


Fig. 4. Comparison between rose diagrams obtained using the VA and SAA for each study area.

A linear feature in CurvaTool philosophy represents a set of clustered points, each characterized by a principal curvature value bigger than the assumed threshold: a line can be fitted on that set, obtaining a direction to North. Therefore, linear features identification comes from a purely geometrical analysis of the DTM: the post-processing of the results, namely the classification of linear features, depends on the purposes of the work and requires the expertise of the user to discard features not representing elements

of interest. Due to the geometrical approach, the quality and the resolution of the DTM, strongly affect the results.

Three DTMs, called following the names of the quarries (Ravaccioni-Fantiscritti, Piastreta, and Piastriccione), containing the same areas as the ones used for the visual approach, were input in CurvaTool code. Each DTM, cut from the regional DTM (GEOscopio, <http://www.regione.toscana.it/-/geoscopio>), represents an area of about 10 km², with an average ground resolution of

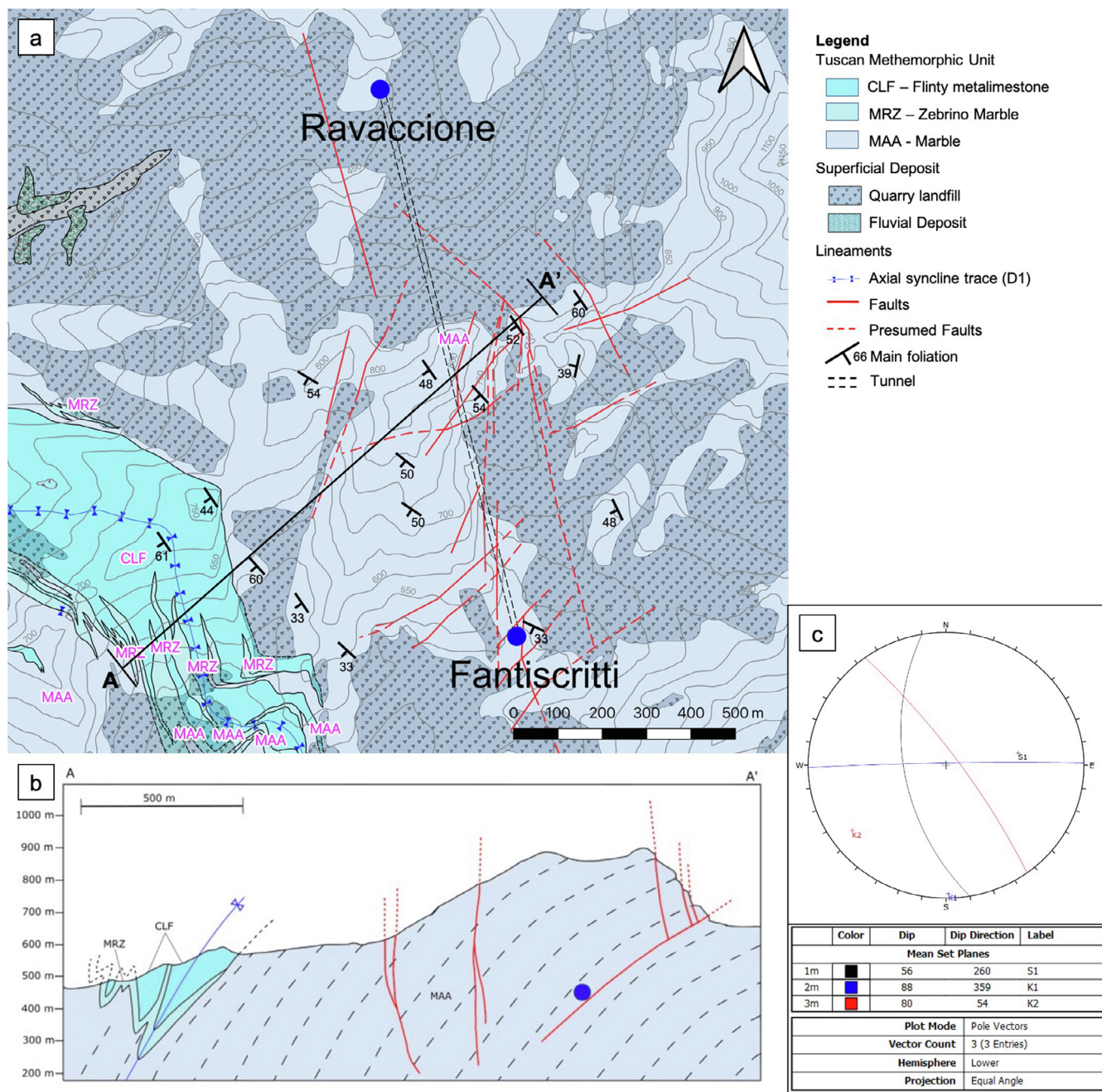


Fig. 5. Geological map (simplified from Mollì et al., 2010) of the Ravaccioni-Fantiscritti basin (a) and cross-section AA' with the location of the quarries (blue circle) (b). Equal angle projection of the main sets measured in the area (c).

10x10m. Results were compared and related to literature data in terms of orientation and corresponding tectonic events.

Sites have been intensely modified by marble exploitation, and the authors would like to test the code to verify its performance also on this kind of area.

3.1.2. The visual approach (VA)

Manual extraction of linear features was performed on the three DTMs and processed with the Line direction Histogram plug-in in

the QGIS environment, which groups the segments according to a selected orientation and visualizes the distribution of segments directions as a rose diagram. The visual approach is based on the experience of the operator. The analysis was based on the observation of the hill-shaded DTMs, their elevation contour maps and available aerial images, in order to show the exact locations of valleys, ridges, and slope breaks and to reduce the effect of the change in the illumination azimuth. The segments representing linear features with potential morpho-tectonic and drainage meaning (such

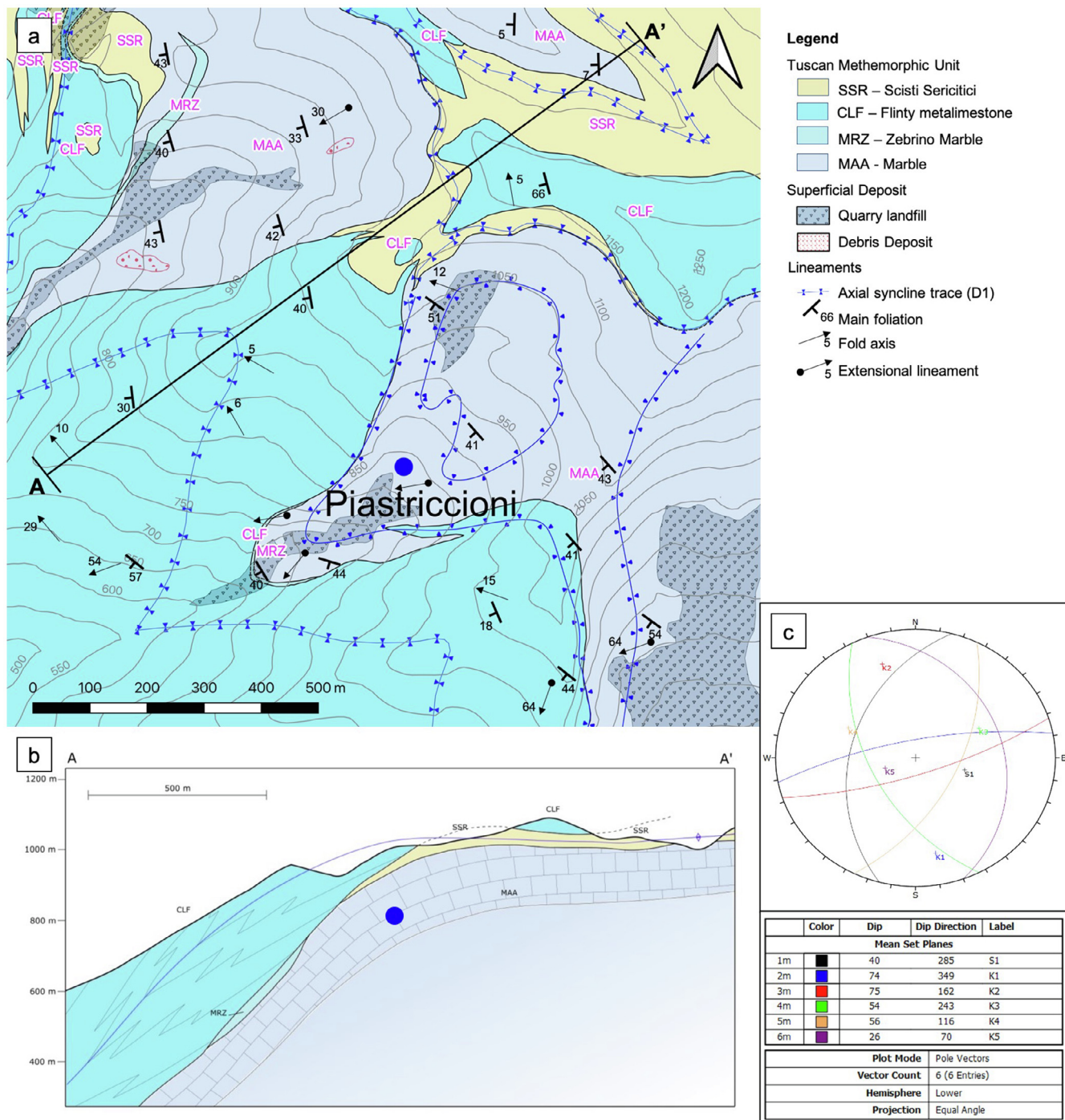


Fig. 6. Geological map (simplified from Vaselli et al., 2007) of the Piastriccioni basin (a) and cross-section AA' with the location of the quarry (b). Equal angle projection of the main sets measured in the area (c).

as rectilinear or segmented patterns of valleys, scarps, ridges, drainage pattern offsets, and stream-segment alignments) were drawn according to the geomorphological criteria. Differences in color tones and light contrasts were also considered in conformity with the tonality criterion. Tonality varies as a function of differences in vegetation, lithology, soil water content, permeability, and rock strength (O’Leary et al., 1976).

While a linear feature simply represents a straight line fitting a set of clustered points geometrically aligned along a specific direction, a lineament takes on a morpho-tectonic meaning (real or

hypothetical), and it is better defined with the geological knowledge of the area (O’Leary et al., 1976).

3.2. Geological and geomechanical survey

In order to characterize quarries materials and the surrounding outcrops, geological and traditional geomechanical surveys were performed according to the *ISRM suggested methods* (1978). In sectors where it was not possible to use scan lines, the window method was used to collect data on discontinuities.

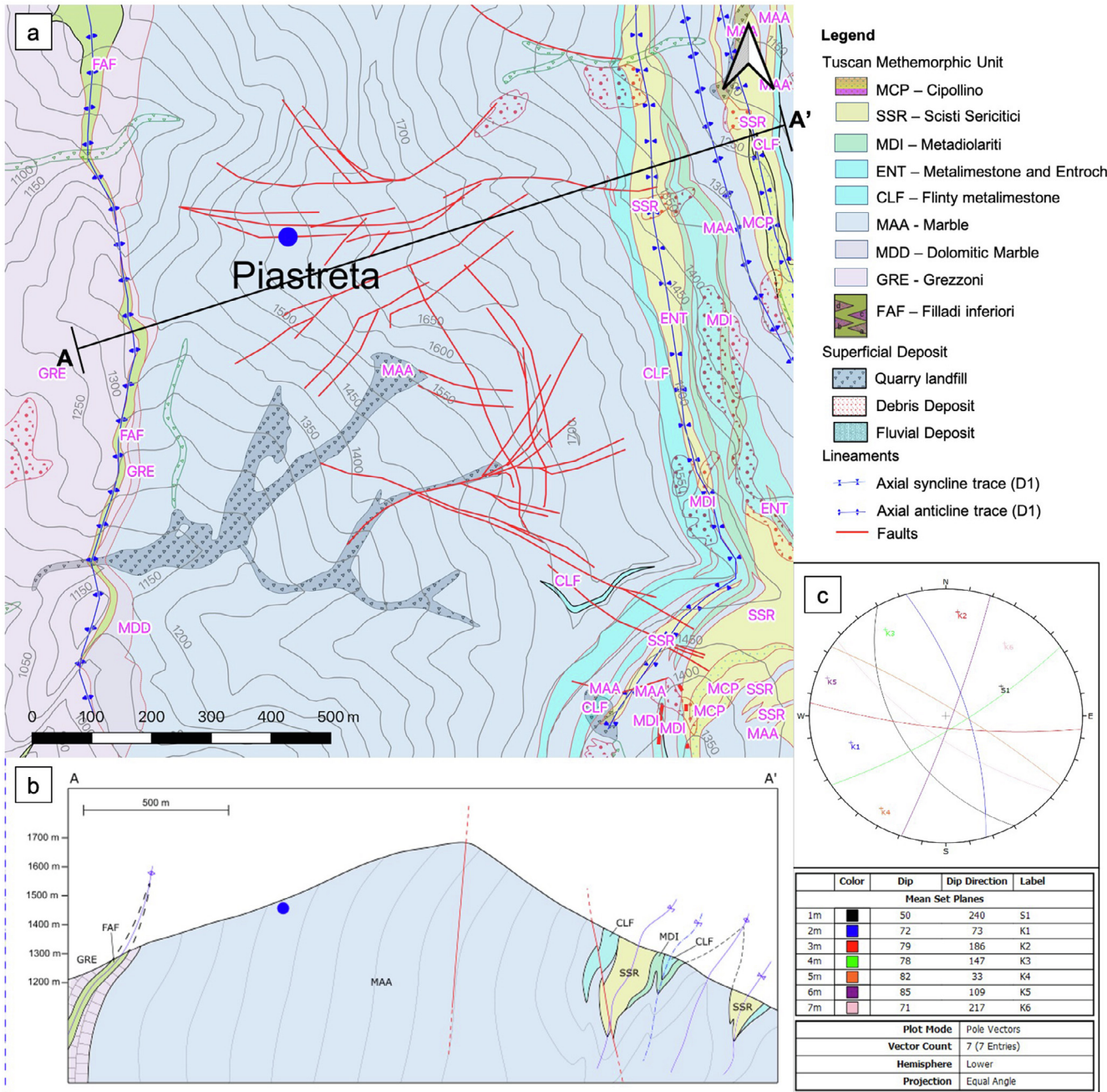


Fig. 7. Geological map (simplified from Carmignani et al., 2003) of the Piastreta basin (a) and cross-section AA' with the location of the quarry (blue circle) (b). Equal angle projection of the main sets measured in the area (c).

Table 2

Principal stress components with mean orientation and intensity for Ravaccioni-Fantiscritti, Piastriccioni and Piastreta quarries.

| Quarry | Borehole | Depth of investigation [m] | Principal stress | Magnitude [MPa] | Plunge [°] | Trend [°] |
|---------------------------|----------|----------------------------|------------------|-----------------|------------|-----------|
| Ravaccione - Fantiscritti | F 01 | 4.27 | σ_1 | 17.4 | 53 | 172 |
| | | | σ_2 | 4.3 | 27 | 40 |
| | | | σ_3 | 2.2 | 23 | 297 |
| | | 7.06 | σ_1 | 10.8 | 46 | 170 |
| | | | σ_2 | 5.2 | 41 | 16 |
| | | | σ_3 | 3.7 | 13 | 274 |
| | F 02 | 6.9 | σ_1 | 16.5 | 79 | 242 |
| | | | σ_2 | 1.3 | 10 | 86 |
| | | | σ_3 | 0.5 | 4 | 355 |
| | | 9.65 | σ_1 | 16.54 | 81 | 293 |
| | | | σ_2 | 2.2 | 9 | 117 |
| | | | σ_3 | 0.6 | 1 | 27 |
| Piastriccioni | | | σ_1 | 10.2 | 61 | 117 |
| | | | σ_2 | 8.5 | 9 | 224 |
| | | | σ_3 | 4.5 | 27 | 318 |
| Piastreta | | 3.8 | σ_1 | 9 | 63 | 106 |
| | | | σ_2 | 2.5 | 23 | 320 |
| | | | σ_3 | 1.6 | 14 | 244 |

Table 3

Comparison between paleostress reconstruction and in-situ stress measurements.

| Quarry | Principal stress | Paleostress | | In-situ measurements | |
|---------------------------|------------------|-------------|-----------|----------------------|-----------|
| | | Plunge [°] | Trend [°] | Plunge [°] | Trend [°] |
| Ravaccione - Fantiscritti | σ_1 | 78 | 47 | 53 | 172 |
| | σ_2 | 10 | 263 | 27 | 40 |
| | σ_3 | 6 | 171 | 23 | 297 |
| | σ_1 | 78 | 47 | 46 | 170 |
| | σ_2 | 10 | 263 | 41 | 16 |
| | σ_3 | 6 | 171 | 13 | 274 |
| | σ_1 | 78 | 47 | 79 | 242 |
| | σ_2 | 10 | 263 | 10 | 86 |
| | σ_3 | 6 | 171 | 4 | 355 |
| | σ_1 | 78 | 47 | 81 | 293 |
| | σ_2 | 10 | 263 | 9 | 117 |
| | σ_3 | 6 | 171 | 1 | 27 |
| Piastriccioni | σ_1 | 63 | 324 | 61 | 117 |
| | σ_2 | 16 | 86 | 9 | 224 |
| | σ_3 | 21 | 182 | 27 | 318 |
| Piastreta | σ_1 | 81 | 263 | 63 | 106 |
| | σ_2 | 6 | 33 | 23 | 320 |
| | σ_3 | 7 | 124 | 14 | 244 |

3.2.1. Estimating stress orientation from geological structures

Many researchers have used faults, folds, joints, dikes, sills, volcanoes, fault striations, or slickensides, as indicators of paleostresses (Price and Cosgrove, 1990). Shape, kinematic pieces of evidence, and geometrical relationships of geological structures allow for the estimation of stress orientation and, at least qualitatively, its magnitude, in terms of a hierarchical classification of principal stresses (Cosgrove and Hudson, 2016).

Three main types of fractures can be recognized: shear fractures, extensional fractures, and hybrid ones. Based on theoretical concepts (Cosgrove and Hudson, 2016), knowing the orientation of the failure surface, the type and direction of the movement, it is possible to infer the original paleostress (Fig. 2).

3.2.2. In situ stress measurements

Theoretically, it is not possible to directly measure the stress state in a rock mass. The prerequisite for the proper evaluation of the virgin stress field is that the measurements are located sufficiently far away from natural boundaries (e.g., rock mass hetero-

geneities, fault zones) or artificial excavation ones. Moreover, the stress measurement is influenced by topography, rock type, heterogeneity, and geological structures.

In this study, the authors used two different techniques for measuring in situ stresses: the CSIRO cells (Ravaccione, Piastreta, and Fantiscritti quarries) and the CSIRO Doorstopper method (Piastriccioni quarry).

Both the methods are based on the principle of over-coring a pilot hole in which measuring strain devices are to be installed. On the hypothesis of continuous, homogeneous, and isotropic rocks and considering the theory of linear elasticity, the strain variation can be used for the determination of the stress field.

The CSIRO triaxial strain cells allow for the complete determination of a stress tensor from a single over-coring operation in one borehole, with the main advantage of drilling of only one borehole for defining the whole stress field. The main limitations are the cost of the cell, the need for long unbroken over-cores, and the long-lasting installing operations.

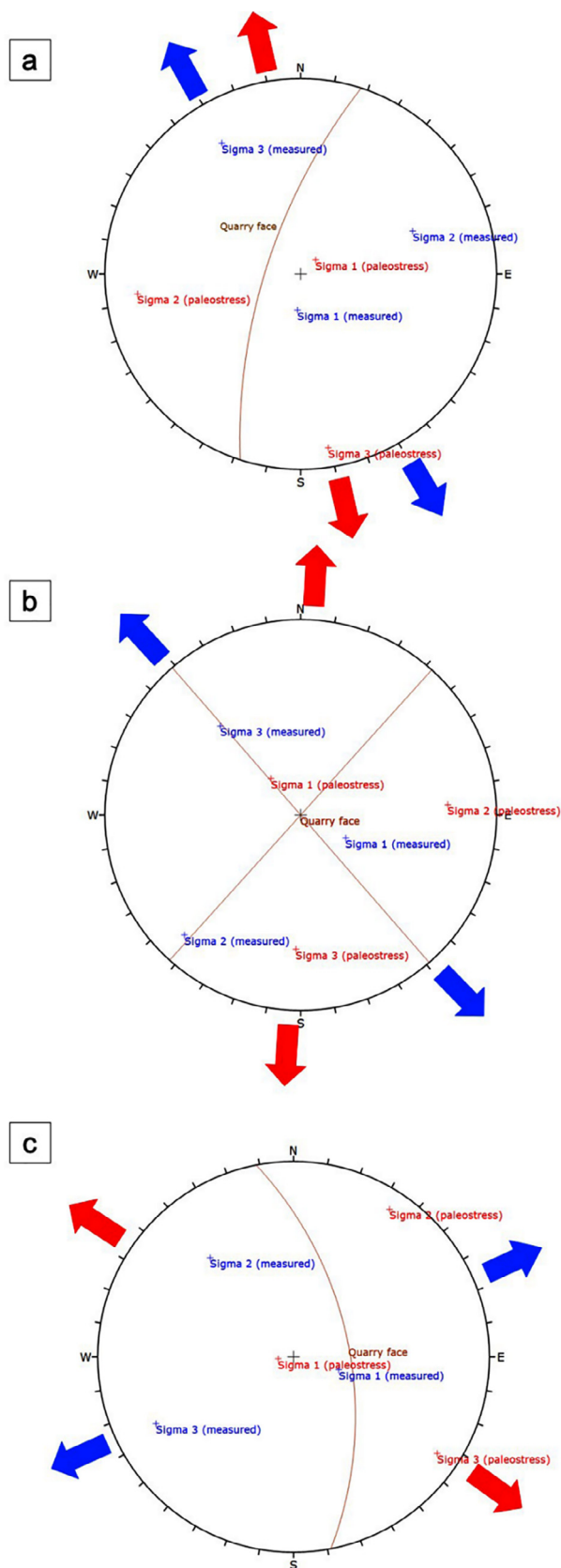


Fig. 8. Trend and plunge representation of the stress tensor, respectively, from in-situ measurement (blue) and far-field interpretation (red) for Ravaccione-Fantiscritti (a), Piastriccioni (b) and Piastrreta (c) quarries. The arrows represent the orientation of σ_3 .

Regarding CSIR Doorstopper cells, a 45 degrees strain rosette consisting of three strain gages is cemented at the base of the borehole. Before and after over-coring, the strain variation is recorded, and the stresses evaluated considering the elastic properties of the rock. The main advantages of this technique are its limited over-core length and the short time for performing the test. The disadvantages are the need for a perfectly flat and smooth surface where to glue the cell, at least three boreholes for the definition of the stress field, and the impossibility of continuous monitoring during over-coring.

4. Results

4.1. Lineament extraction

The main results of linear feature extraction obtained with VA and SAA methods are shown in Fig. 3 and detailed in Table 1.

The frequency and orientation of the linear features identified in each macro-area are plotted in rose diagrams (Fig. 4). The two approaches show a quite coherent trend distribution of the main linear features. In general, the three regions are characterized by four main trends (NNE-SSW, NE-SW, NW-SE, and E-W to ENE-WSW). They match the orientation of the main geological structures associated with D1 and D2. This coherence supports the assumption that those linear features represent the morphotectonic expression of regional and local structures and represent potential geological lineaments. Some differences in frequency are observed comparing the two approaches. In detail:

In the Ravaccione-Fantiscritti area, lineaments follow three main orientations: NNE-SSW (high frequency both in VA and SAA), NE-SW (more evident in VA), and NW-SE.

In the Piastriccioni area, both the approaches highlight three main trends: NNE-SSW (the most frequent), NW-SE and E-W.

In the Piastrreta area, NNE-SSW trending linear features are the most abundant. NW-SE and E-W trends are highlighted, particularly in SAA, although they are present in small percentages.

4.2. Local geological and geomechanical surveys

Geological information and geomechanical data were collected in each quarry site. Most of the surveyed fractures are associated with the orientations of the main faults.

Fractures are sensitive markers of stress change and occur pervasively in shallow tectonic environments; therefore, they are considered as stress indicators (Pollard and Segall, 1987; Arlegui and Simón, 2001).

4.2.1. Ravaccione - Fantiscritti site

The Ravaccione and Fantiscritti quarries are located in the Fantiscritti mining district. They are geologically situated at the core of the Carrara Syncline (Fig. 5a). The exploited marble belongs to the Marmi s.s. Formation (MAA in Fig. 5b) and shows the main bedding, S0, and the main schistosity, S1, WSW-dipping at medium-high dip (260/56).

Two main fracture sets were recognized in the quarry (Fig. 5c), respectively NW-SE and E-W oriented.

4.2.2. Piastriccioni quarry

The Piastriccioni Quarry is located in the Pescina Boccanaglia mining district, in the northwesternmost part of the Carrara Basin. In this district, the Marmi s.s. Formation outcrops in correspon-

dence of the normal and reverse limb of the Carrara Syncline (Fig. 6a and 6b).

The S1 schistosity is W-dipping with a NNW-SSE direction (N300), and six sets of fractures have been censused, representing three sets of conjugate fractures trending NE-SW, NW-SE, and NNE-SSW (Fig. 6c).

4.2.3. Piastreta quarry

The Piastreta quarry is in the Piastreta-Sella mining district. The quarry is situated in the reverse limb of the Monte Tamburna Anticline (Fig. 7a). The “Marble” Formation outcrops in the area (Fig. 7b) with the original bedding (S0) and the main schistosity (S1) dipping to W with NNE-SSW direction (N15). The D1 event caused isoclinal folds with N-S striking axial plane W-dipping; the D2 stage produced only a bland waving of the main schistosity S1 at the mesoscale.

Besides the main schistosity, five fracture sets were identified in the quarry (Fig. 7c), indicating three different systems (NE-SW, NW-SE, and E-W) with conjugate fractures each.

4.3. In situ stress measurements

In Ravaccione and Fantiscritti quarries, four in situ stress measurements with CSIRO cells were carried out in correspondence of two horizontally drilled boreholes (F01 and F02) (Ferrero et al., 2013; Alejano et al., 2017).

F02 is oriented NS in correspondence of an EW trending quarry face, whereas F01 is NNW-SE striking, and the rock face is NE-SW oriented.

In the Piastreta quarry, the CSIRO cell was installed inside a horizontal borehole E-W oriented (trend and plunge of 80 degrees and 3 degrees, respectively). The rock face is NNW-SSE striking, perpendicular to the borehole.

In the Piastriccioni quarry, doorstopper cells were installed in 3 boreholes with orientation varying from N-S to WNW-ESE.

The results in terms of main orientations and intensities for each area are reported in Table 2.

5. Discussions

Trends of the linear features are quite coherent in VA and SAA. They are consistent with the main directions of the geological structures associated with the deformational events reported in the literature (Carmignani and Kligfield, 1990; Molli et al., 2002; Ottria and Molli, 2000).

The high number of NNE-SSW trending ones, detected by both VA and SAA, is justified by the presence of both D1 and D2 structures with similar orientations: axial planes of early D2 folds, normal and oblique-normal D2 faults and sinistral strike-slip D1 faults show such trend.

The NW-SE trending linear features, particularly evident in the semi-automatic approach, match the direction of both the axial plane of D1 isoclinal folds and the dextral strike-slip faults associated with the brittle D1 deformation.

The E-W average trend detected by the semi-automatic method is coherent with local E-W trending D1 reverse faults and ENE-WSW (up to NE-SW) trending D2 normal to oblique-normal faults (Molli et al., 2010).

Modification of the morphology due to the quarry activities, which hide the evidence of the morphotectonic control, together with the subjectivity of the operator, conditioned the number of linear features detected (significantly lower in VA) and the relative frequency of the main trends.

Trends similar to those of linear features have been locally identified in the quarries during geomechanical surveys, attesting the coherence of the mesoscale fractures with regional structures, and lineaments obtained from DTM processing (Fig. 3). Geometrical features and kinematics indicators of those fractures help in the reconstruction of the local natural stress and the relationship with the far-field paleostress.

The structural associations in the Ravaccione - Fantiscritti quarries is represented by two main sets of fractures, NW-SE and NE-SW to ENE-WSW oriented. These orientations are coherent with the D1 strike-slip faults and the D2 normal to normal-oblique regional faults, which are linked to a vertical maximum stress, σ_1 , and horizontal intermediate and minimum stress, σ_3 , NNW-SSE trending.

In the Piastriccioni quarry, the NW-SE and NE-SW trending fractures show geometrical similarity with the D1 strike-slip faults. In contrast, the E-W to WNW-ESE trending and the NNE-SSW striking fractures are coherent to the D2 normal and oblique normal faults. All those structures suggest a local vertical maximum stress (σ_1), horizontal intermediate (σ_2), and minimum stress (σ_3), respectively oriented about E-W and N-S.

In the Piastreta quarry, superimposed D1/D2 structures are present with NW-SE and E-W trending fractures connected to strike-slip and reverse D1 brittle structures, in association with NE-SW and ENE-WSW striking sets linked with the regional D2 normal faults system (Molli and Vaselli, 2006). Such structures are coherent with a final extensional stress field, with sub-vertical σ_1 and sub-horizontal σ_2 and σ_3 , respectively NW-SE and NE-SW trending.

All local natural stress fields are in accordance with the far-field paleostress reported in Ottria and Molli (2000) that reported two major groups of tensors. The first one, linked to the compressional tectonic stage, is characterized by a vertical intermediate stress (σ_2), a sub-horizontal N-S oriented principal stress (σ_1), and a minor E-W trend stress (σ_3). The second one, associated with the extensional stage, is represented by a vertical σ_1 , a sub-horizontal N-S oriented σ_2 , and an E-W to NE-SW trending σ_3 .

The in-situ stress measurements record the influence of the quarry activities, which becomes progressively weaker going far from the rock mined faces (particularly evident in the Ravaccioni-Fantiscritti quarries, where deeper measurements were carried out in the same borehole, Table 2). In Table 3, in-situ stress measurements are compared with the local stress field resulting from both geological and geomechanical field surveys and literature (Ottria and Molli, 2000).

In Fantiscritti (Fig. 8a), σ_1 changes from N47 to N170 trend with a plunge reduction, becoming quite parallel to the rock face, whereas σ_3 rotates up to a WNW-ESE trend (from N171 to N297), which corresponds to the perpendicular to the rock face. Both σ_2 and σ_3 show a little increase in the plunge values.

In Ravaccione (Fig. 8a), the quarry face was already oriented nearly parallel and perpendicular to the maximum and minimum paleostress tensors, respectively. Arrangements in σ_1 and σ_3 are observed with the vertical σ_1 paleostress changing in trend from about N47 to N293 and the horizontal σ_2 and σ_3 rotating of about 180 degrees.

In Piastriccioni (Fig. 8b), σ_1 just modifies the trend from N263 to N106, maintaining a quite vertical plunge, whereas σ_3 and σ_2 rotate of about 40 degrees counterclockwise. The σ_3 and σ_2 are reoriented perpendicularly to the NE-SW and NW-SE face, respectively.

In Piastreta (Fig. 8c), σ_1 maintains the original vertical orientation with a change in the trend (from N86 to N263) and the horizontal σ_3 and σ_2 just rotate of about 60 degrees

counterclockwise, standing the σ_3 nearly perpendicular to the quarry face.

6. Conclusions

Geological structures could represent useful indicators of paleostress and are fundamental for the far-field definition. The analysis at the mesoscale of the orientation, kinematic, and geometrical properties of the geological structures allows for the estimation of stress orientation and, at least, qualitatively, the hierarchical classification of principal local stresses.

Field data also allowed to associate similar kinematic indicators to specific sets of structural elements that can be identified at local and regional scale in relation to the different deformational events of the area.

The rapid development and affordability of the products, the need to work on big areas, even not accessible, and the (semi-) automatic processing allow for the use of remotely sensed data for multiscale approaches, integrating regional data to field survey observations, usually limited to the accessible areas. In particular, the remote sensing helps to recognize the presence, at a regional scale, of morphotectonic structures with geometrical features similar to those recognized at the local scale on the field and associated to specific kinematic meanings. This furnishes a more detailed framework for the far-field definition, particularly where scarce literature data are available.

Moreover, the visual approach in the image analysis is strongly subjective and depends on the experience of the operator: the possibility to operate with automatic or semi-automatic techniques in the interpretation of the DTM features offers the opportunity to improve the objectivity of the processing at the regional scale.

The proposed methodology is extremely versatile since it allows the determination of the direction and (at least qualitatively) the amount of the stress state at basin scale by using different types of remotely sensed image (satellite or aerial images) and data (LIDAR). This information can be coupled by field surveys and stress measurements in order to validate the hypotheses made and to quantify the stress state tensor acting in that area.

In underground works, the natural stress state changes according to the design and development of excavation. To avoid stability problems, in situ measurements and numerical models must be produced during the design and monitoring, to guarantee safety conditions and the knowledge of the far-field results fundamental to set a correct numerical model and define the variations of the local stress produced by the excavation at the time of the measurements.

Declaration of Competing Interest

The authors declare that they have no known competing financial interests or personal relationships that could have appeared to influence the work reported in this paper.

References

Alejano, L.R., Castro-Filgueira, U., Ferrero, A.M., Migliazza, M., Vagnon, F., 2017. In situ stress measurement near fault and interpretation by means of discrete element modelling. *Acta Geodyn. Geomater.* 14, 181–194. <https://doi.org/10.13168/AGG.2017.0002>.

Al-Obeidat, F., Feltrin, L., Marir, F., 2016. Cloud-based Lineament Extraction of Topographic Lineaments from NASA Shuttle Radar Topography Mission Data. *Procedia Comput. Sci.* 83, 1250–1255. <https://doi.org/10.1016/j.procs.2016.04.260>.

Amadei, B., Stephansson, O., 1997. *Rock Stress and Its Measurement*. Springer Netherlands, Dordrecht. <https://doi.org/10.1007/978-94-011-5346-1>

Angelier, J., 1994. *Fault slip analysis and paleostress reconstruction*. In: Hancock, P. L. (Ed.), *Continental Deformation*. Pergamon Press, Oxford, pp. 53–100.

Arlegui, L., Simón, J.L., 2001. Geometry and distribution of regional joint sets in a non-homogeneous stress field: case study in the Ebro basin (Spain). *J. Struct. Geol.* 23 (2–3), 297–313. [https://doi.org/10.1016/S0191-8141\(00\)00097-3](https://doi.org/10.1016/S0191-8141(00)00097-3).

Bonetto, S., Facello, A., Umili, G., 2017. A New Application of CurvaTool Semi-Automatic Approach to Qualitatively Detect Geological Lineaments. *Environ. Eng. Geosci.* 23 (3), 179–190. <https://doi.org/10.2113/gseengeosci.23.3.179>.

Bonetto, S., Facello, A., Umili, G., 2020. The contribution of CurvaTool semi-automatic approach in structural and groundwater investigations. A case study in the Main Ethiopian Rift Valley. *Egypt. J. Remote Sens. Sp. Sci.* 23 (1), 97–111. <https://doi.org/10.1016/j.ejrs.2018.10.003>.

Carmignani, L., Kliffeld, R., 1990. Crustal extension in the northern Apennines: The transition from compression to extension in the Alpi Apuane Core Complex. *Tectonics* 9 (6), 1275–1303. <https://doi.org/10.1029/TC009i006p01275>.

Carmignani, L.; Antompaoli, M.L.; Fantozzi, P.L.; Meccheri, M., 2003. Studi conoscitivi sui bacini marmiferi industriali di Carrara: un contributo per la gestione pianificata dell'attività. Tav. 3 - Carta delle varietà merceologiche dei bacini marmiferi del Carrarese. *Quaderni Studi Documentali*, GEAM 24.

Célérier, B., Etchecopar, A., Bergerat, F., Vergely, P., Arthaud, F., Laurent, P., 2012. Inferring stress from faulting: From early concepts to inverse methods. *Tectonophysics* 581, 206–219. <https://doi.org/10.1016/j.tecto.2012.02.009>.

Cosgrove, J.W., Hudson, J.A., 2016. *Structural geology and rock engineering*. Imperial College Press, London, UK.

Ferrero, A.M., Migliazza, M., Segalini, A., Gulli, D., 2013. In situ stress measurements interpretations in large underground marble quarry by 3D modeling. *Int. J. Rock Mech. Min. Sci.* 60, 103–113. <https://doi.org/10.1016/j.ijrmm.2012.12.008>.

Ferrero, Anna Maria, Umili, Gessica, Vagnon, Federico, 2016. Analysis of discontinuity data obtained with remote sensing tools to generate input for EC7 design. *Rock Mechanics and Rock Engineering: From the Past to the Future* 2, 1115–1120. <https://doi.org/10.1201/9781315388502-194>.

Fossen, H., 2016. *Structural geology*. Cambridge University Press, Cambridge, UK.

Ganas, A., Pavlides, S., Karastathis, V., 2005. DEM-based morphometry of range-front escarpments in Attica, central Greece, and its relation to fault slip rates. *Geomorphology* 65 (3–4), 301–319. <https://doi.org/10.1016/j.geomorph.2004.09.006>.

ISRM, 1978. *Commission on standardization of laboratory and field tests. Suggested methods for the quantitative description of discontinuities in rock masses*. *Int. J. Rock Mech. Min. Sci. Geomech. Abs.* 15, 319–368.

Jacques, P.D., Machado, R., Nummer, A.R., 2012. A comparison for a multiscale study of structural lineaments in southern Brazil: LANDSAT-7 ETM+ and shaded relief images from SRTM3-DEM. *An. Acad. Bras. Ciênc.* 84 (4), 931–942. <https://doi.org/10.1590/S0001-37652012000400008>.

Lisle, R., Orife, T., Arlegui, L., 2001. A stress inversion method requiring only fault slip sense. *J. Geophys. Res.* 106 (B2), 2281–2289. <https://doi.org/10.1029/2000JB900353>.

Maerten, L., Maerten, F., Lejri, M., Gillespie, P., 2016. Geomechanical paleostress inversion using fracture data. *J. Struct. Geol.* 89, 197–213. <https://doi.org/10.1016/j.jsg.2016.06.007>.

Masoud, A.A., Koike, K., 2011. Auto-detection and integration of tectonically significant lineaments from SRTM DEM and remotely-sensed geophysical data. *ISPRS J. Photogramm. Remote Sens.* 66 (6), 818–832. <https://doi.org/10.1016/j.isprsjprs.2011.08.003>.

Molli, G., Vaselli, L., 2006. Structures, interference patterns, and strain regime during midcrustal deformation in the Alpi Apuane (Northern Apennines, Italy), in: *Styles of Continental Construction*. Geological Society of America, pp. 79–93. [https://doi.org/10.1130/2006.2414\(05\)](https://doi.org/10.1130/2006.2414(05))

Molli, G., Giorgetti, G., Meccheri, M., 2002. *Tectono-metamorphic evolution of the Alpi Apuane metamorphic complex: New data and constraints for geodynamic models*. *Boll. Soc. Geol. Ita.* 1, 789–800.

Molli, G., Cortecci, G., Vaselli, L., Ottria, G., Cortopassi, A., Dinelli, E., Mussi, M., Barbieri, M., 2010. Fault zone structure and fluid–rock interaction of a high angle normal fault in Carrara marble (NW Tuscany, Italy). *J. Struct. Geol.* 32 (9), 1334–1348. <https://doi.org/10.1016/j.jsg.2009.04.021>.

O'Leary, D.W., Friedman, J.D., Pohn, H.A., 1976. Lineament, linear, lineation: Some proposed new standards for old terms. *Geol. Soc. Am. Bull.* 87, 1463. [https://doi.org/10.1130/0016-7606\(1976\)87<1463:LLSPN>2.0.CO;2](https://doi.org/10.1130/0016-7606(1976)87<1463:LLSPN>2.0.CO;2)

Ottria, G., Molli, G., 2000. Superimposed brittle structures in the late-orogenic extension of the Northern Apennine: results from the Carrara area (Alpi Apuane, NW Tuscany). *Terra Nov.* 12, 52–59. <https://doi.org/10.1111/j.1365-3121.2000.00272.x>

Pollard, D.D., Segall, P., 1987. Theoretical displacements and stresses near fractures in rock: with applications to faults, joints, veins, dikes, and solution surfaces. In *Fracture Mechanics of Rocks*. Academic Press, London, pp. 277–347.

Price, N.J., Cosgrove, J.W., 1990. *Analysis of geological structures*. Cambridge University Press, Cambridge, UK.

Ramli, M.F., Yusof, N., Yusoff, M.K., Juahir, H., Shafri, H.Z.M., 2010. Lineament mapping and its application in landslide hazard assessment: a review. *Bull. Eng. Geol. Environ.* 69 (2), 215–233. <https://doi.org/10.1007/s10064-009-0255-5>.

- Rawnsley, K.D., Rives, T., Petti, J.-P., Hencher, S.R., Lumsden, A.C., 1992. Joint development in perturbed stress fields near faults. *J. Struct. Geol.* 14 (8-9), 939–951. [https://doi.org/10.1016/0191-8141\(92\)90025-R](https://doi.org/10.1016/0191-8141(92)90025-R).
- Seleem, T.A., 2013. Analysis and Tectonic Implication of DEM-Derived Structural Lineaments, Sinai Peninsula. *Egypt. Int. J. Geosci* 04 (01), 183–201. <https://doi.org/10.4236/ijg.2013.41016>.
- Soto-Pinto, C., Arellano-Baeza, A., Sánchez, G., 2013. A new code for automatic detection and analysis of the lineament patterns for geophysical and geological purposes (ADALGEO). *Comput. Geosci.* 57, 93–103. <https://doi.org/10.1016/j.cageo.2013.03.019>.
- Umili, G., Bonetto, S., Ferrero, A.M., 2018. An integrated multiscale approach for characterization of rock masses subjected to tunnel excavation. *J. Rock Mech. Geotech. Eng.* 10 (3), 513–522. <https://doi.org/10.1016/j.jrmge.2018.01.007>.
- Vaz, D.A., Di Achille, G., Barata, M.T., Alves, E.I., 2012. Tectonic lineament mapping of the Thaumasia Plateau, Mars: Comparing results from photointerpretation and a semi-automatic approach. *Comput. Geosci.* 48, 162–172. <https://doi.org/10.1016/j.cageo.2012.05.008>.